Evaluation of Plasma and Warm Dense Matter Transport Coefficient Models for High Energy Density Applications

High Energy Density Science Seminar

Oleg Schilling
Lawrence Livermore National Laboratory

22 February 2024

LLNL-PRES-860553
This work was performed under the auspices of the U.S. Department of Energy by Lawrence Livermore National Laboratory under contract DE-AC52-07NA27344. Lawrence Livermore National Security, LLC

Lawrence Livermore National Laboratory

Topics to be discussed

- Introduction and motivation
  - high energy density applications
  - effects of including/excluding plasma transport in ICF-relevant hydrodynamic flows
  - multicomponent diffusion
- Plasma and warm dense matter transport coefficient models
  - model inputs
  - general structure of models
  - summary of models
- `Jupyter/Python` package
  - capabilities
  - purpose
- Model applications and intercomparisons
  - examples of binary mixing of D-T, D-C, D-Al, and D-Au
  - examples of single-component mixing of D
- Summary, conclusions, and future work

Introduction and Motivation

Warm dense matter (WDM) and plasma transport (mass diffusion, viscous dissipation, and thermal conduction) are important in HED applications

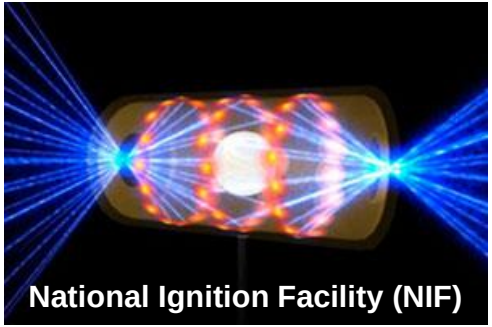

- Accurate models for electron thermal conduction are crucial
- Plasma viscosity and diffusivity reduce hydrodynamic instability growth and smooth fluctuations

- Accurate models for electron thermal conduction and electric conductivity are crucial
- Plasma viscosity and diffusivity reduce hydrodynamic instability growth and smooth fluctuations

- Accurate models for mass diffusion and electron thermal conduction are crucial
- Diffusion is central to `purification' of white dwarf atmospheres through gravitational sedimentation of heavy elements such as ^{22}Ne

The inclusion or exclusion of transport physics has important implications

- Describe physics of atomic scale mass diffusion, viscous dissipation, and thermal diffusion
- Molecular transport terms affect linear and nonlinear hydrodynamic instability growth
  - provide stabilizing mechanisms
  - needed for transition to turbulence
- Transport coefficient values set important length- and timescales, and dimensionless numbers
  - characteristic dissipation and diffusion length- and timescales
  - Schmidt, Prandtl, Lewis, Reynolds, Péclet numbers
- When averaged equations are solved (e.g., large-eddy simulation or turbulence models), models for unresolved hydrodynamics should vanish in direct numerical simulation (DNS) limit
  - molecular transport terms needed for stability and to represent correct small-scale physics in this limit
- Wave (e.g., shock) propagation is affected by molecular transport

It is likely that some discrepancies between HED simulation and experimental results are attributable to exclusion of plasma transport or to the use of inaccurate transport coefficients

A series of papers by Vold and collaborators (2014–2021) examined the implications of including plasma transport in ICF-relevant simulations

- xRAGE code simulations of single-mode Rayleigh–Taylor and Kelvin–Helmholtz instability with and without plasma viscosity and diffusivity show that
  - plasma transport smooths flow fields
  - reduces small-scale structure
  - reduces instability growth

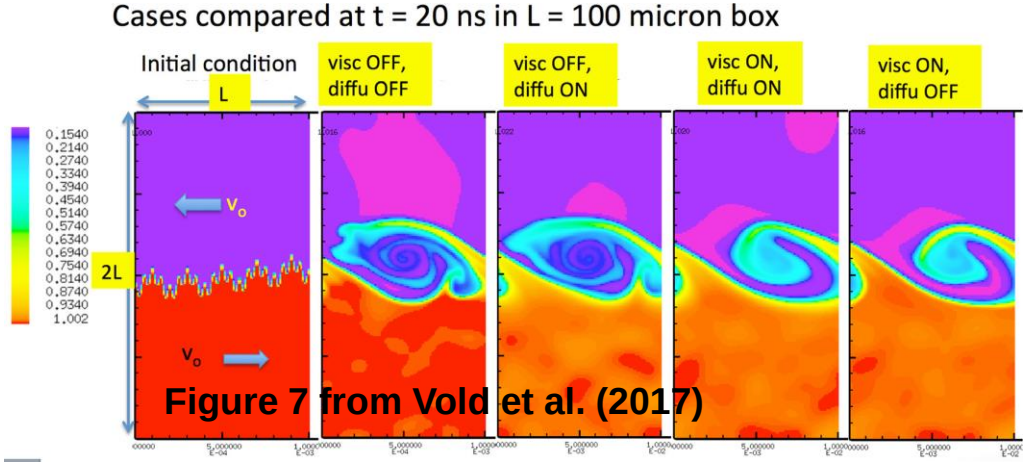

Figure 7 from Vold et al. (2017)

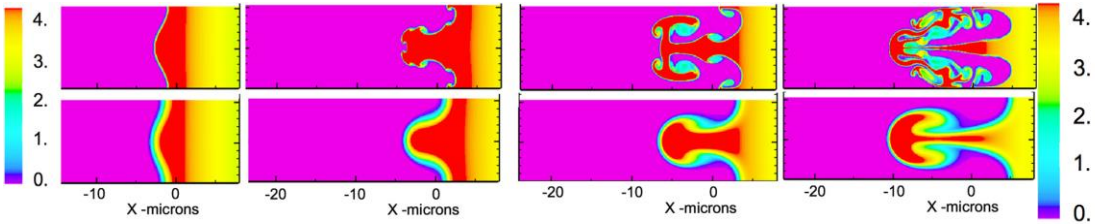

Figure 6 from Vold, Yin & Albright (2021)

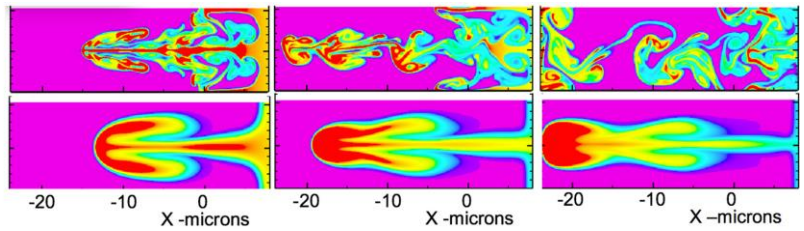

Figure 7 from Vold, Yin & Albright (2021)

Viscous dissipation and mass diffusion are mechanisms that reduce hydrodynamic instability growth and smooth fluctuations

- Consider ICF deceleration example of Vold, Yin and Albright (2021)
- Rayleigh–Taylor instability growth rate with viscosity, diffusivity, and a diffusion layer is

$$\omega(k) = \sqrt{\frac{g\,At\,k}{1 + b\,k\,\delta(t)} + \left[\left(\nu_{12} + D_{12}\right)k^2\right]^2} - \left(\nu_{12} + D_{12}\right)k^2$$

$$\delta(t) = 2\sqrt{D_{12}\,t}$$

- Viscosity, diffusivity, and diffusion layer damp ideal growth rate, which now has a maximum value
- Evaluate coefficients for a D-C mixture taking t = 0.2 ns
- As T increases, maximum value decreases and peak moves to smaller wavenumbers (longer wavelengths)
- Growth rate is very small at highest temperatures

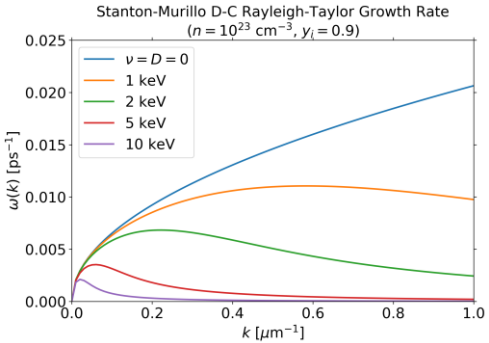

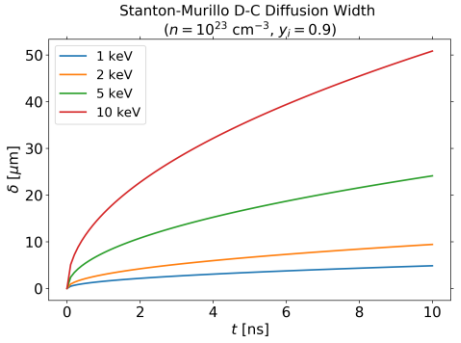

- Diffusion widths corresponding to these temperatures increase faster with time at higher T
- Spatial profiles of D mass fraction are wider (more diffuse) at higher T

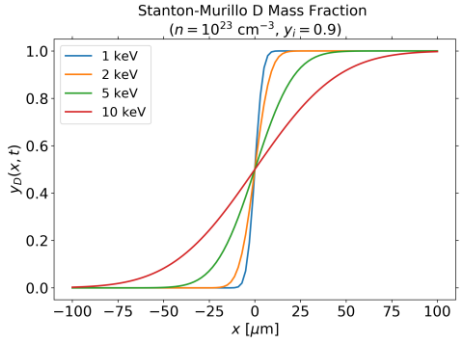

$$y_D(x,t) = \frac{1}{2}\left\{1 + \mathrm{erf}\left[\frac{x}{2\sqrt{D_{12}\,t}}\right]\right\}$$

Atomic transport in dense ion/electron plasmas is complicated and very different from molecular transport in gases and liquids

- Classical fluid dynamics treatments of liquids and gases only require constant or relatively simple transport coefficients
  - incompressible flows usually have constant coefficients
  - compressible flows usually have temperature-dependent coefficients (e.g., Sutherland's law, $\propto T^{0.7}$), particularly important for combustion thermodynamics
- Transport coefficients for WDM and plasmas are significantly different
  - coefficients depend on charge states, atomic numbers, masses, and fractions, densities, temperature etc., and are different for ions and electrons
  - derived using kinetic theory (e.g., a perturbative treatment of Boltzmann equations for ion and electron distribution functions using a *Chapman–Enskog expansion*) or calculated numerically using *molecular dynamics* (MD) and parameterized
  - coefficient values can change by orders of magnitude within diffusion (mixing) layers
  - weakly- and strongly-coupled (high and low temperature) regimes must be considered in general

A physically correct treatment of plasma transport requires consideration of multicomponent diffusion, which is a complicated subject

Multicomponent Diffusion

- Species mass fraction, momentum, and species internal energy equations are

$$\frac{\partial}{\partial t}(\rho\, y_r) + \frac{\partial}{\partial x_j}(\rho\, y_r\, v_j) = R_r - \frac{\partial J_r}{\partial x_j}$$

$$\frac{\partial}{\partial t}(\rho\, v_i) + \frac{\partial}{\partial x_j}(\rho\, v_i\, v_j) = F_i - \frac{\partial p}{\partial x_i} + \frac{\partial}{\partial x_j}\left[\rho\, \nu_{rs}\left(\frac{\partial v_i}{\partial x_j} + \frac{\partial v_j}{\partial x_i} - \frac{2}{3}\,\delta_{ij}\,\frac{\partial v_k}{\partial x_k}\right)\right]$$

binary viscosity ν_{rs}

$$\frac{\partial}{\partial t}(\rho\, U_r) + \frac{\partial}{\partial x_j}(\rho\, U_r\, v_j) = S_r + \rho\, c_v \sum_s \frac{T_s - T_r}{\tau_{rs}} + \frac{\partial}{\partial x_j}\left(\rho\, c_p\, \chi_{rs}\, \frac{\partial T_r}{\partial x_j}\right)$$

binary thermal diffusivity χ_{rs}

- Kinetic theory shows that mass diffusion flux $J_i^r = \rho_r\,(v_i^r - v_i)$ is more general than Fickian: depends on ion/electron pressures and temperatures, and on species fractions for a multicomponent plasma*

$$\mathbf{J}_r = -\rho\, D_{rs}\,[\ \underbrace{\nabla y_r}_{\text{Fickian diffusion}} + \underbrace{(x_r - y_r)\,\nabla \ln p_i + (z_r - y_r)\,\frac{\nabla p_e}{p_i}}_{\text{barodiffusion}} + \underbrace{k_i^{T,r}\,\nabla \ln T_i + k_e^{T,r}\,\frac{\nabla T_e}{T_i}}_{\text{thermodiffusion}}\ ]$$

binary mass diffusivity D_{rs}

*Nomenclature: species *r, s*; ion and electron pressure p_i and p_e; ion and electron temperature T_i and T_e; number fraction $x_r = n_r/n$; mass fraction $y_r = \rho_r/\rho$; charge fraction $z_r = n_r Z_r/n_e$; thermodiffusion ratios $k_{i,e}^{T,r}$

Summary of Plasma and Warm Dense Matter Transport Coefficient Models

Plasma transport coefficient models require many quantities* depending on species densities, temperature, mean ionizations, screening etc., as well as on collision integrals

- Particle interactions are described by a *Yukawa (screened Coulomb) pair potential* with *Debye–Hückel screening length*

$$\Phi_{rs}(r) = \frac{Z_r\, Z_s\, e^2}{r}\, \mathrm{e}^{-r/\lambda_{DH}} \quad , \quad \lambda_{DH}(T_e, T_i) = \sqrt{\frac{k_B}{4\,\pi\, e^2\, (n_e/T_e + \sum_r n_r\, Z_r^2/T_i)}}$$

- *Plasma coupling parameter* and *dimensionless inverse effective screening length*

$$\Gamma_{rs}(T) = \frac{Z_r\, Z_s\, e^2}{a_{tot}\, k_B\, T} \quad , \quad \kappa = \frac{a_{tot}}{\lambda_{\mathrm{eff}}}$$

- *Total ion-sphere radius* and *Fermi energy* (with *electron number density* $n_e = \sum_r Z_r\, n_r$)

$$a_{tot} = \left(\frac{4}{3}\,\pi\, n\right)^{-1/3} \quad , \quad E_F = \frac{\hbar^2}{2\, m_e}\left(3\,\pi^2\, n_e\right)^{2/3}$$

- *Binary collision integrals* are a function of *cross-sections* and *scattering angle*

$$\Omega_{rs}^{(n,m)}(T) = \sqrt{\frac{k_B\, T}{2\pi\, m_{rs}}} \int_0^\infty V^{2m+3} \exp\left(-V^2\right) \sigma_{rs}^{(n)}(V)\, \mathrm{d}V \quad , \quad V \equiv \sqrt{\frac{m_{rs}\, v^2}{2\, k_B\, T}}$$

$$\sigma_{rs}^{(n)}(v) = 2\pi \int_0^\infty b\left\{1 - \cos^n\left[\theta_{rs}(b,v)\right]\right\} \mathrm{d}b \quad , \quad \theta_{rs}(b,v) = \pi - 2\, b \int_{r_0}^\infty \frac{\mathrm{d}r}{r^2 \sqrt{1 - (b/r)^2 - 2\,\Phi_{rs}(r)/(m_{rs}\, v^2)}}$$

*Nomenclature: species *r*, *s*; Boltzmann constant k_B; electron and ion temperature T_e and T_i; electron, ion, and total ion number density n_e, n_r, and n; reduced mass m_{rs}; effective charge Z_r; impact parameter *b*

Most plasma transport coefficient models originate from kinetic theory developed by Chapman, Cowling, and Enskog over 100 years ago for weakly-coupled systems

- Binary mass diffusivity, dynamic (shear) viscosity, thermal conductivity, and thermodiffusion ratio*

$$D_{rs} = \frac{3\,k_B\,T}{16\,n\,m_{rs}\,\Omega_{rs}^{(1,1)}}$$

$$\mu_{rs} \equiv \rho\,\nu_{rs} = \frac{x_r^2\,R_r + x_s^2\,R_s + x_r\,x_s\,R'_{rs}}{x_r^2\,R_r/\mu_r + x_s^2\,R_s/\mu_s + x_r\,x_s\,R_{rs}}$$

$$K_{rs} \equiv \rho\,c_{p,rs}\,\chi_{rs} = \frac{x_r^2\,Q_r\,K_r + x_s^2\,Q_s\,K_s + x_r\,x_s\,Q'_{rs}}{x_r^2\,Q_r + x_s^2\,Q_s + x_r\,x_s\,Q_{rs}}$$

$$k_{rs}^T \equiv \frac{D_{rs}^T}{D_{rs}} = \frac{5\,C\,x_r\,x_s\,(x_r\,S_r - x_s\,S_s)}{x_r^2\,Q_r + x_s^2\,Q_s + x_r\,x_s\,Q_{rs}}$$

Quantities in these expressions are functions of collision integrals, temperature, and other factors

Principal differences between models are:
1) choice of effective screening length λ_{eff}
2) evaluation of collision integrals

- Single-component mass diffusivity, dynamic viscosity, and thermal conductivity

$$D_r = \frac{3\,k_B\,T}{8\,n\,m_r\,\Omega_{rr}^{(1,1)}} \quad , \quad \mu_r \equiv \rho_r\,\nu_r = \frac{5\,k_B\,T}{8\,\Omega_{rr}^{(2,2)}} \quad , \quad K_r \equiv \rho_r\,c_{p,r}\,\chi_r = \frac{25\,c_{v,r}\,k_B\,T}{16\,\Omega_{rr}^{(2,2)}}$$

*Nomenclature: species r, s; Boltzmann constant k_B; temperature T; number density n; reduced mass m_{rs}; collision integrals $\Omega_{rs}^{(n,m)}$; number density fractions $x_r = n_r/n$

In general, the models require expressions for effective screening lengths, coupling parameters, and collision integrals*

- For Chapman–Cowling model, only *collision integral* needed

$$\Omega_{rs}^{(1,1)} = \pi \left(\frac{Z_r \, Z_s \, e^2}{2 \, k_B \, T} \right)^2 \sqrt{\frac{k_B \, T}{2\pi \, m_{rs}}} \ln\left(1 + v_{01}^2\right) \quad , \quad v_{01}(T) = \frac{4 \, \lambda_{DH} \, k_B \, T}{Z_r \, Z_s \, e^2}$$

ratio of Debye–Hückel length and distance of closest approach

- For Paquette et al. model of a binary ionic mixture, *collision integral* is (c_{in} are spline coefficients)

$$\Omega_{rs}^{(1,1)} = \pi \left(\frac{Z_r \, Z_s \, e^2}{2 \, k_B \, T} \right)^2 \sqrt{\frac{k_B \, T}{2\pi \, m_{rs}}} \times \exp\left\{ c_{1n}^{(1)} \left[\psi_{rs}(n+1) - \psi_{rs}\right]^3 + c_{2n}^{(1)} \left[\psi_{rs} - \psi_{rs}(n)\right]^3 + c_{3n}^{(1)} \left[\psi_{rs}(n+1) - \psi_{rs}\right] + c_{4n}^{(1)} \left[\psi_{rs} - \psi_{rs}(n)\right] \right\}$$

with independent variables for spline fits

$$\psi_{rs}(T) = \ln\left[\ln\left(1 + \gamma_{rs}^2\right)\right] \quad , \quad \gamma_{rs}(T) \equiv \frac{4 \, \lambda_{\text{eff}} \, k_B \, T}{Z_r \, Z_s \, e^2}$$

and *effective screening length* (maximum of ion-sphere radius and Debye–Hückel length)

$$\lambda_{\text{eff}} = \max\left(a_{tot}, \lambda_{DH}\right)$$

or improved expression (Fontaine et al. 2015)

$$\lambda_{\text{eff}} = \frac{\lambda_{DH}^5 + a_{tot}^5}{\lambda_{DH}^4 + a_{tot}^4}$$

In general, the models require expressions for effective screening lengths, coupling parameters, and collision integrals

- For Stanton–Murillo model of a binary ionic mixture, *effective screening length* is (with $p = 9/5$)

$$\lambda_{\rm eff} = \left[\frac{1}{\lambda_e^2} + \sum_{r=1}^{2} \frac{1}{\lambda_r^2 \left(1 + 3\,\Gamma_r^{IS}\right)} \right]^{-1/2} \quad , \quad \lambda_e = \lambda_{TF} \quad , \quad \lambda_r = \lambda_{DH} \quad , \quad a_r = \left(\frac{4\,\pi}{3\,Z_r} \sum_{s=1}^{2} Z_s\, n_s \right)^{-1/3}$$

- *Single species (ion-sphere) and effective coupling parameters* are

$$\Gamma_r^{IS} = \frac{Z_r^2\, e^2}{a_r\, k_B\, T} \quad , \quad g_{rs}(T) = \frac{Z_r\, Z_s\, e^2}{\lambda_{\rm eff}\, k_B\, T}$$

- *Collision integrals* are parameterized and expressed in weak-coupling (WC) $g_{rs} < 1$ and strong-coupling (SC) $g_{rs} > 1$ regimes

$$\Omega_{rs}^{(n,m)}(T) = \sqrt{\frac{2\pi}{m_{rs}}}\, \frac{\left(Z_r\, Z_s\, e^2\right)^2}{\left(k_B\, T\right)^{3/2}}\, K_{nm}(g_{rs}) \quad , \quad K_{nm}(g_{rs}) = \begin{cases} K_{nm}^{WC}(g_{rs}) & \text{if } g_{rs} < 1 \\ K_{nm}^{SC}(g_{rs}) & \text{if } g_{rs} > 1 \end{cases}$$

$$K_{nm}^{WC}(g_{rs}) \approx -\frac{n}{4}\,(m-1)!\,\ln \sum_{k=1}^{5} a_k\, g_{rs}^k \quad , \quad K_{nm}^{SC}(g_{rs}) \approx \frac{b_0 + b_1\,\ln(g_{rs}) + b_2\,\ln(g_{rs})^2}{1 + b_3\, g_{rs} + b_4\, g_{rs}^2}$$

$\{a_k\}$ and $\{b_k\}$ are tabulated coefficients

The Molvig–Simakov–Vold (2014) model* for ion diffusivities, viscosities, and conductivities in plasmas is one of the most comprehensive kinetic theory models available

- *Binary interdiffusion coefficient* is

$$D_{iI} = \alpha_{11}(\Delta_I)\,\frac{m_I}{m_i\,Z_I^2}\,D_p\,\frac{(k_B\,T_i)^{5/2}}{\rho_i\,A_i^{1/2}}\,\frac{y_i}{y_I}\quad,\quad D_p = \frac{2112.77}{\ln\Lambda}\qquad \ln\Lambda(T) = \ln\left[1+\frac{0.014\,T_i\,\sqrt{T_e}}{z_r\,z_s\,\sqrt{n_r\,Z_r + n_s\,Z_s}}\right]$$

where *Onsager transport matrix element* and *ion coupling (or scattering) parameter* is

$$\alpha_{11}(x) = \frac{3\pi}{128}\,\frac{288+604\,\sqrt{2}\,x+217\,x^2}{72+61\,\sqrt{2}\,x+16\,x^2}\quad,\quad \Delta_I(y_i) = \frac{n_I\,Z_I^2}{n_i} = \frac{m_i\,Z_I^2}{m_I}\,\frac{1-y_i}{y_i}$$

- *Light ion dynamic (shear) viscosity* is

$$\mu_i = \frac{3\pi\,\sqrt{2}}{32}\,\alpha_\mu(\Delta_I)\,\Delta_I\,n_i\,m_i\,D_{iI}\quad,\quad \alpha_\mu(\Delta_I) = \frac{5}{6\,\sqrt{2}}\,\frac{205\,\sqrt{2}+408\,\Delta_I}{178+301\,\sqrt{2}\,\Delta_I+192\,\Delta_I^2}$$

- *Light ion thermal conductivity* is

$$K_i = \lim_{\Delta_I\downarrow 0} n_i\,m_i\,c_{v,i}\,D_{iI}\,\alpha_2^i(\Delta_I)\quad,\quad \alpha_2^i(\Delta_I) = \frac{25}{4}\,\alpha_{22}(\Delta_I) + \frac{15}{4}\,y_I\left(1-\frac{m_i}{m_I}\right)\alpha_{12}(\Delta_I)$$

There is considerable uncertainty in the Coulomb logarithm

*Nomenclature: light and heavy ions *i*, *I*; Boltzmann constant k_B; electron and ion temperature T_e and T_i; mass fraction y_r; ion mass m_r; A_i light ion atomic mass; effective charge Z_r ; Coulomb logarithm $\ln\Lambda$; number density n_r; light ion specific heat at constant volume $c_{v,i}$

The warm dense matter (WDM) regime is very challenging to understand and model

- Regime can be defined generally by a range in temperature–density–pressure space
  - temperatures ~5 × (10^3–10^6) K (~0.5–500 eV)*
  - densities ~10^{-2}–10^4 g/cm^3
  - pressures ~1 Mbar–500 Gbar
- Relevant to ICF capsule implosions, white dwarfs, and some planetary cores
- WDM is difficult to probe experimentally, simulate, and model
  - electrons are *degenerate* (p = 9/5):

$$\Theta(T_e) = \frac{k_B\,T_e}{E_F} \approx 0.1\text{–}1 \quad , \quad \Gamma_{ee}(T_e) = \frac{e^2}{a_e\left[(k_B\,T_e)^p + E_F^p\right]^{1/p}} \lesssim 10$$

  - quantum effects are important

*upper bound on temperature is often taken to be lower, ~100 eV

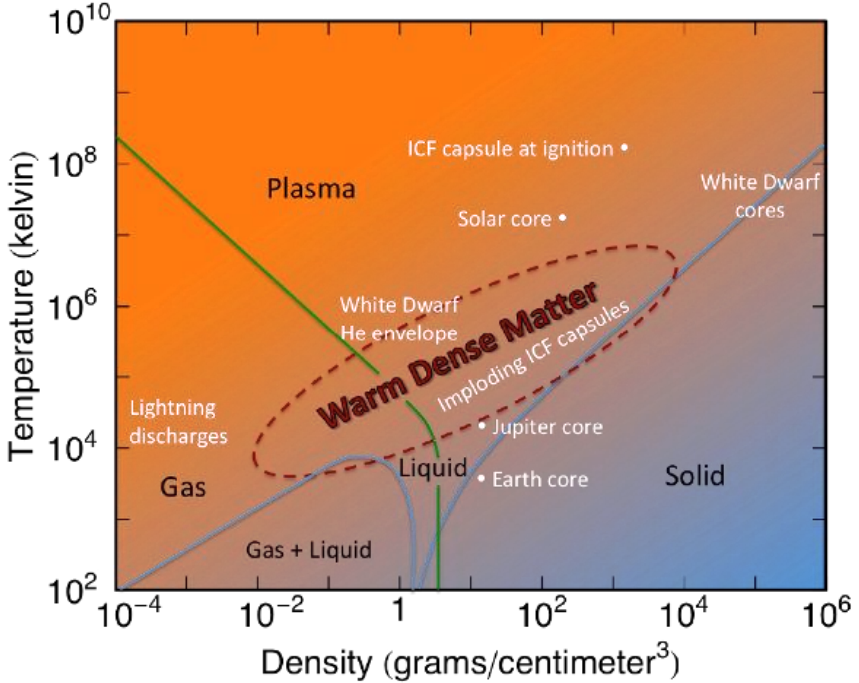

Figure 1 from "Basic Research Needs for High Energy Density Laboratory Astrophysics", Report of the Workshop on HEDLP Research Needs, 15–18 November 2018, Department of Energy

Most warm dense matter transport coefficient models originate from a combination of kinetic theory and molecular dynamics data for strongly-coupled systems

- Described by a *normalized temperature* (T_m is *melt temperature* or *melt boundary*), Murillo (2008) *Einstein frequency* (from a fit to MD data) and *ion plasma frequency* ($\kappa = a/\lambda_{TF}$)

$$T^* = \frac{T}{T_m} = \frac{\Gamma_m}{\Gamma} \quad , \quad \omega_E(\kappa) = \frac{\omega_i}{\sqrt{3}} \exp\left(-0.2\,\kappa^{1.62}\right) \quad , \quad \omega_i = \sqrt{\frac{4\,\pi\,n\,Z^2\,e^2}{m_i}}$$

- Ohta–Hamaguchi (2000) self-diffusivity model is (with tabulated values of α, β, and γ)

$$D(\kappa) = \left[\alpha(\kappa)\,(T^* - 1)^{\beta(\kappa)} + \gamma(\kappa)\right] \omega_E(\kappa)\,a^2$$

- Murillo (2008) Yukawa viscosity model is a reparameterization of Saigo–Hamaguchi (2002) model

$$\mu(T^*) = \left(0.0051\,T^* + \frac{0.374}{T^*} + 0.022\right) \sqrt{3}\,m_i\,n\,\omega_E(\kappa)\,a^2 \quad , \quad \Gamma_m(\kappa) = 171.8{+}82.8\left[\exp\left(0.565\,\kappa^{1.38}\right) - 1\right]$$

- Caplan–Bauer–Freeman (2022) self-diffusivity model is (with specified functions *A*, *B*, and *C*)

$$D(\Gamma,\kappa) = \sqrt{\frac{\pi}{3}}\,\frac{A(\kappa)\,\mathrm{e}^{-B(\kappa)\Gamma}}{\Gamma^{5/2}\ln\left[1 + C(\kappa)/\left(\sqrt{3}\,\Gamma^{3/2}\right)\right]}\,\omega_i\,a^2$$

Modern large-scale molecular dynamics (MD) simulations can calculate transport coefficients with fewer assumptions than needed in analytic kinetic theory models

- When bare Coulomb charges scatter, $1/r$ interaction introduces a *Coulomb logarithm* in scattering integrals, $\ln\Lambda = \ln(b_{max}/b_{min})$
  - logarithm of ratio of long-range screening to short-range quantum effects (without such effects, integrals diverge)
  - in weakly-coupled regime where ion kinetic energy dominates potential energy, kinetic theory is accurate
  - kinetic theory predictions are much less accurate in strongly-coupled regime because of uncertainty in $\ln\Lambda$
- MD simulations can calculate plasma transport coefficients in both weakly- and strongly-coupled regimes
  - MD simulations do not require approximations such as binary only collisions, weak-coupling, or small-angle scattering
  - large-angle scattering and spatial correlations of ions and electrons are incorporated by directly integrating particle equations of motion
  - MD also includes quantum electronic effects such as charge screening and degeneracy arising from Pauli exclusion principle

Juypter/Python Package for Model Implementation and Analysis

A `Jupyter` notebook package was developed to compute single-component and binary transport coefficients using the previously discussed models

- Inputs are atomic masses/numbers, number densities, temperature, mean ionization states etc.
- Computes plasma parameters (screening lengths, plasma couplings etc.)
- Prints values of key intermediate quantities for reference
- `Matplotlib` used to rapidly plot quantities
- Equations and explanatory text implemented in `Markdown` for integrated documentation
- Emphasis is on clarity, transparency, reproducibility, flexibility

- Serves many purposes
  - provide coefficient values and trends to develop understanding and help explain physics
  - provide estimates of coefficients: how similar/different are they from liquid and gas values?
  - provide estimates of dimensionless numbers: how similar/different are they from liquid and gas values?
  - rapidly implement new/modified models, and perform model-to-model or model-to-data comparisons
  - use for code verification: are models implemented correctly?
  - could be used to provide dynamic estimates in simulations

This package helps remove the “black box” aspects of these models

The package currently includes many kinetic theory-based and molecular dynamics-informed models

- Kinetic theory models
  - Chapman–Cowling (1939) single-component and binary ionic D (1st and 2nd order), ν, χ; k^T
  - Molvig–Simakov–Vold (2014) binary ionic D, ν, χ and electronic χ
- Molecular dynamics-informed models
  - Paquette et al. (1986) single-component and binary ionic D (1st and 2nd order), ν, χ; k^T; Fontaine et al. (2015) correction
  - Ohta–Hamaguchi (2000) single-component ionic D
  - Saigo–Hamaguchi (2002) single-component ionic ν
  - Murillo (2008) single-component and binary [one-component plasma (OCP)] ionic ν; Rudd (2012) correction
  - Stanton–Murillo (2016) single-component and binary ionic D (1st and 2nd order), ν, χ; k^T
  - Caplan–Bauer–Freeman (2022) single-component and binary (OCP) ionic D
- Other models
  - Binary thermal diffusion ratio $(3/2)(x_r - z_r^2)$
  - Generalized Sutherland ν
  - Power-law D, ν, χ

It will be assumed in all calculations that ions and electrons are in temperature equilibrium $T_i = T_e = T$

The mean ionization state of each species is calculated using the Thomas–Fermi (TF) model for binary mixtures

- For a partially-ionized, multicomponent system, *mean ionization state* of each species is $Z_r = Z_{TF}(1/V_r, Z_{nuc,r}, T_e)$ (V_r is ion-sphere volume associated with *r*th species in presence of other species)
  - reduced volume is calculated by setting $V_r/Z_r = V_s/Z_s$ for each species pair subject to $\sum_r n_r V_r = 1$
  - thus, a binary system requires solution of

$$Z_1 = Z_{TF}(1/V_1, Z_{nuc,1}, T_e) \quad , \quad Z_2 = Z_{TF}(1/V_2, Z_{nuc,1}, T_e)$$

$$n_1 V_1 + n_2 V_2 = 1 \quad , \quad \frac{V_1}{Z_1} = \frac{V_2}{Z_2}$$

  which can be solved iteratively until convergence achieved
- However, TF model is not accurate for WDM: ionization should be calculated using an average-atom model, for example

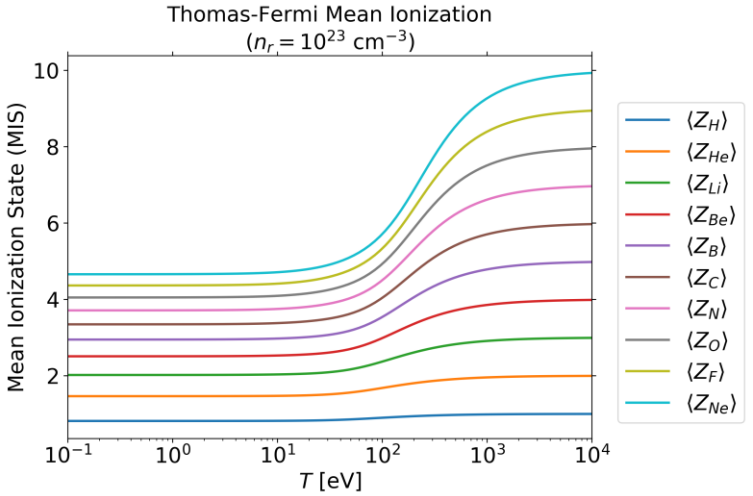

Low *Z* elements approach full ionization at lower temperatures, while high *Z* elements require progressively higher temperatures for full ionization [see Stanton, Glosli & Murillo (2018)]

An approximate fit to the Thomas–Fermi effective charge was given by More (1985) to avoid inline computational expense

- Mean ionization state can be defined using electron number density evaluated at ion-sphere radius, $Z_{TF} = Z_{nuc} - (4\pi/3)\, a_r^3 n_e(a_r)$ (Z_{nuc} is bare nuclear charge)
- An approximate fit to $Z_{TF}(n_r, Z_{nuc}, T_e)$ was given:

$$Z_{TF} = \frac{x}{1 + x + \sqrt{1 + 2x}}\, Z_{nuc}$$

$$x = \alpha_1\, Q^{\alpha_2} \quad , \quad Q = \left(R^C + Q_1^C\right)^{1/C} \quad , \quad Q_1 = A\, R^B \quad , \quad C = k_7\, T_f + k_8$$

$$B = -\exp\left(k_4 + k_5\, T_f + k_6\, T_f^7\right) \quad , \quad A = k_0\, T_0^{k_1} + k_2\, T_0^{k_3} \quad , \quad T_f = \frac{T_0}{1 + T_0}$$

$$T_0 = \frac{T_e}{Z_{nuc}^{4/3}} \quad , \quad R = \frac{n_i}{Z_{nuc}\, N_A}$$

with coefficients

$$\alpha_1 = 14.3139 \quad , \quad \alpha_2 = 0.6624 \quad , \quad k_0 = 3.323 \times 10^{-3} \quad , \quad k_1 = 0.9718\,,$$

$$k_2 = 9.26148 \times 10^{-5} \quad , \quad k_3 = 3.10165 \quad , \quad k_4 = -1.7630\,,$$

$$k_5 = 1.43175 \quad , \quad k_6 = 0.31546 \quad , \quad k_7 = -0.366667 \quad , \quad k_8 = 0.983333$$

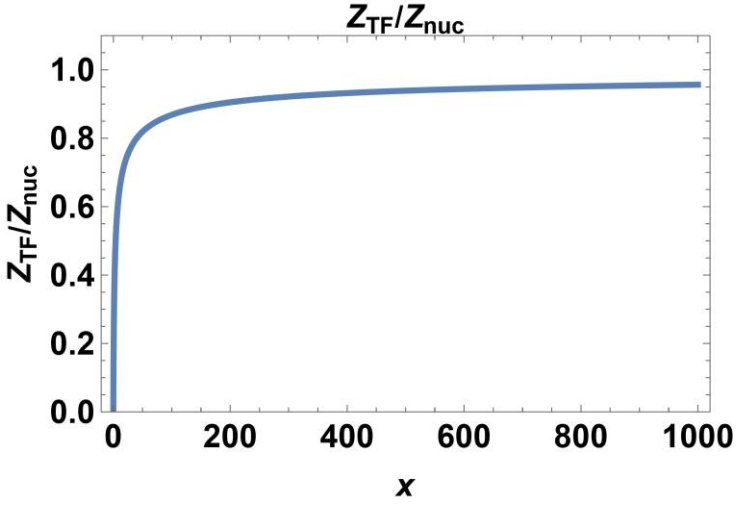

- N_A is Avagadro's number, ionic number density n_r [1/cm³], and T_e [eV]

Model Applications and Model Intercomparisons

As increasingly asymmetric in Z mixtures are considered, higher temperatures are needed to achieve full ionization $\langle Z_r(T)\rangle \rightarrow Z_{nuc,r}$

- Mean ionization state is T- and n-dependent
  - lighter ions (D, C) fully ionize at 10 keV
  - heavier ions (Al, Au) still partially ionized at 10 keV
  - higher $Z \rightarrow$ higher T needed for full ionization
- Many applications:
  - specify some average constant values
  - use $Z_{nuc,r}$ (assume full ionization)
  - use simplified TF approach for each species separately
- Note on temperature range:
  1 eV ≈ 11,600 K so
  $T = 1.16 \times 10^3 - 1.16 \times 10^8$ K

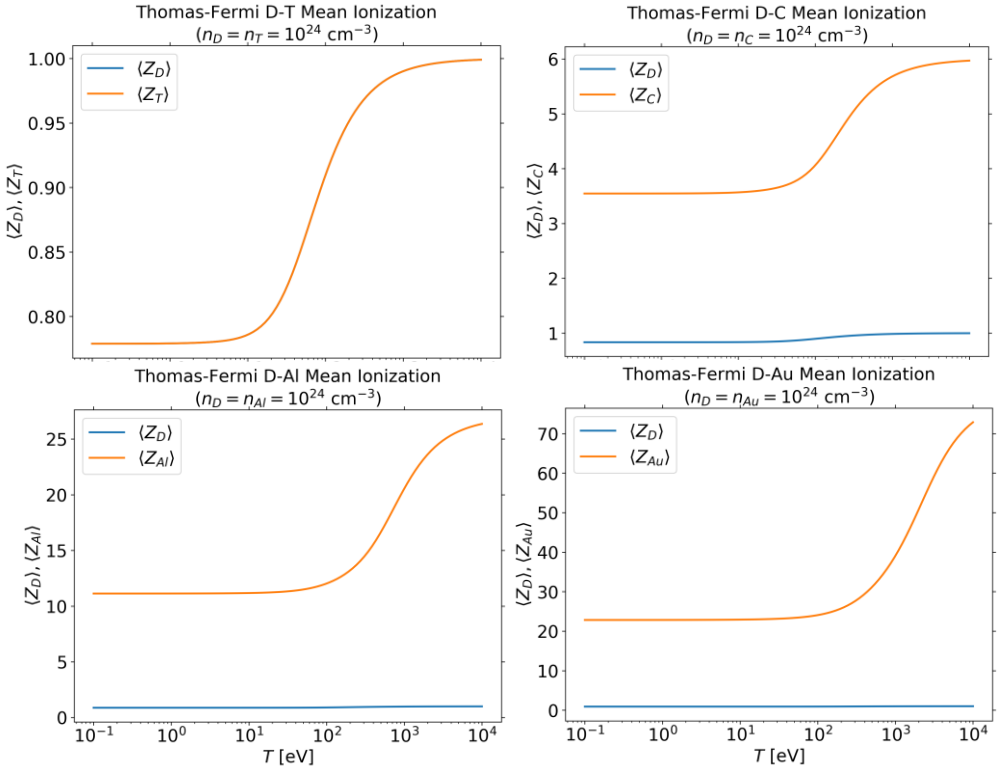

As increasingly asymmetric in Z mixtures are considered, the mass interdiffusivity has a shallower and lower dependence on temperature

- Light ion mixture (D-T) has highest values at high T and lowest values at low T
  - scales as $\propto T^{5/2}$ at high T (classical Braginskii weakly-coupled scaling)
  - values range over 6 orders of magnitude
  - virtually no dependence on mass fraction
- With a higher asymmetry (D-C and D-Al), high T scaling $\propto T^2$
- At highest asymmetry (D-Au), scaling is $\propto T$ at high T
- As asymmetry increases
  - interdiffusivities attain minimum values at higher T
  - have a much stronger dependence on y_i
  - attain larger values at lower T

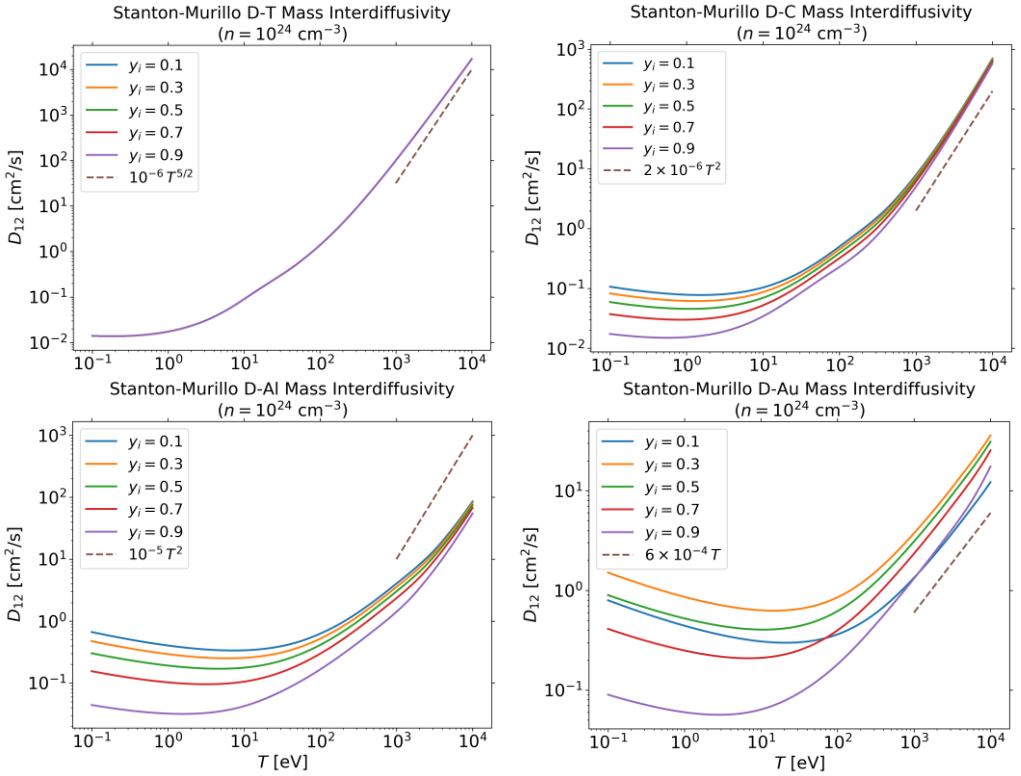

As increasingly asymmetric in Z mixtures are considered, the binary kinematic viscosity has a shallower and lower dependence on temperature

- Most general trends are same as for interdiffusivities
- As asymmetry increases
  - high T scaling progresses from $\propto T^{5/2}$, to $\propto T^2$, to $\propto T$
  - viscosities attain minimum values
  - have a much stronger dependence on y_i
  - attain larger values at lower T
- An important difference from behavior of interdiffusivities is that viscosity values maintain separation for different y_i over all T for D-C, D-Al, and D-Au

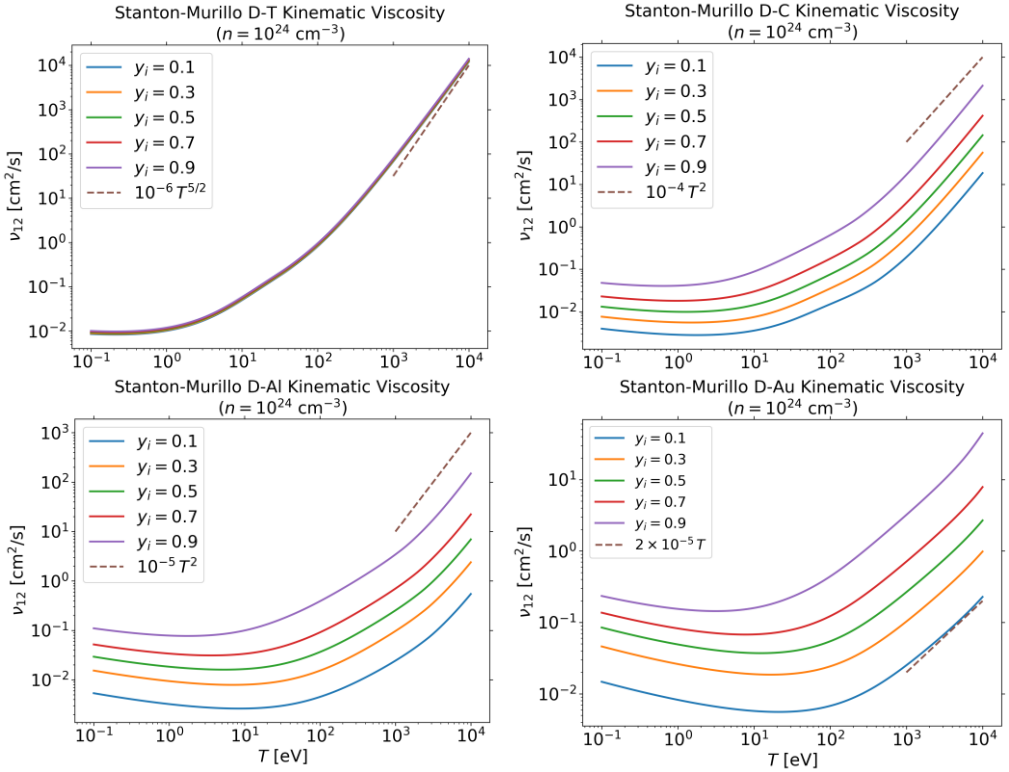

The Schmidt numbers $Sc = \nu/D$ range from ~10^{-2} to ~6 over the entire range of temperature, composition, and Z asymmetry

- For this number density, values are < 1 except for $y_i = 0.9$
- Range of values becomes very strongly dependent on Z asymmetry and y_i
  - for D-T, $Sc \in [0.55, 0.8]$
  - for D-C, D-Al, and D-Au, Sc ranges over orders of magnitude for different y_i
  - Sc decreases with increasing Z asymmetry
- Values are remarkably nearly constant over this wide range in T
  - ν_{rs} and D_{rs} both have nearly same T-dependence
  - using a constant value is a very good approximation for a given y_i

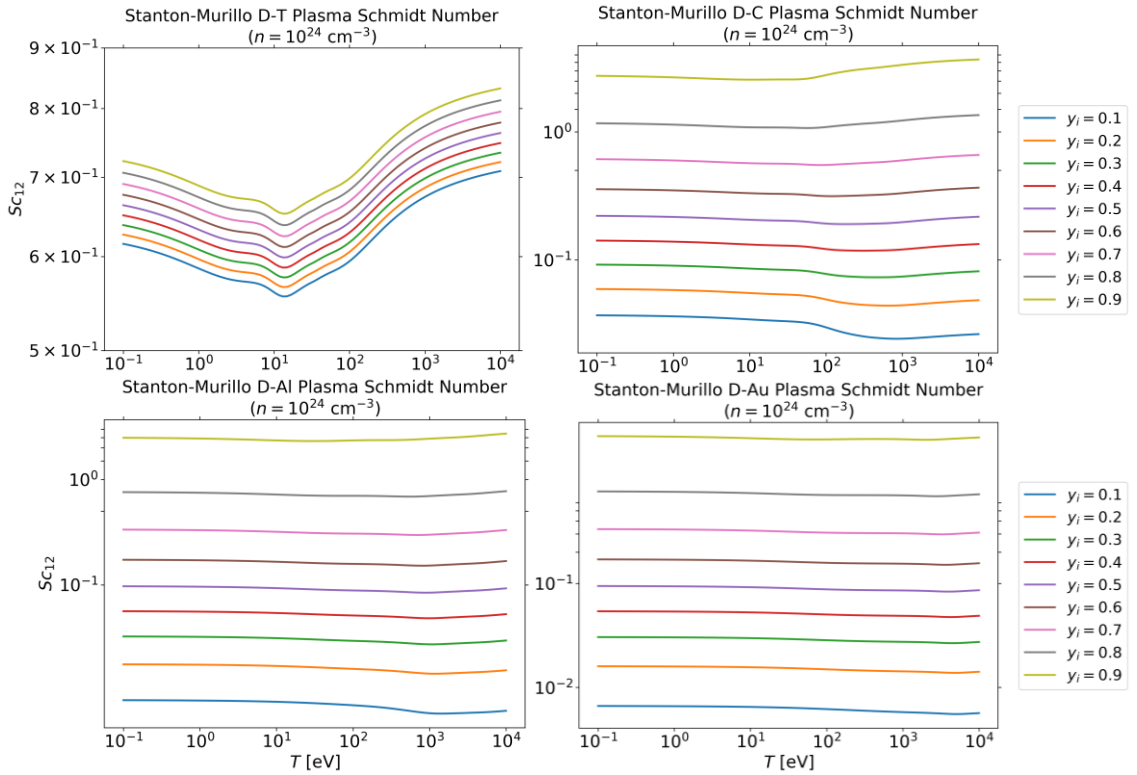

The mixture mass interdiffusivities are increasingly divergent as charge asymmetry increases (Z_1 = 1 for D, Z_2 = 1 for T → 79 for Au) and number density increases (n = 10^{24} → 10^{29} cm^{-3})

- For D-T with n = 10^{24} cm^{-3}, models agree well at high T, but can differ by orders of magnitude at low T
- Except for D-Au case with n = 10^{29} cm^{-3}, models scale $\propto T^{5/2}$ at high T
- For larger n, Molvig–Simakov–Vold model is orders of magnitude larger than other models at high temperatures
  - Stanton–Murillo and Paquette et al. models agree closely at highest temperatures
  - Caplan–Bauer–Freeman is orders of magnitude smaller for D-Au
- Values are reduced by orders of magnitude as n increases by 5 orders of magnitude
- *For D-Au with n = 10^{24} and 10^{29} cm^{-3}, values are completely different*
- These represent extreme applications of models that were not originally developed for such low temperatures, high densities, and large Z asymmetries

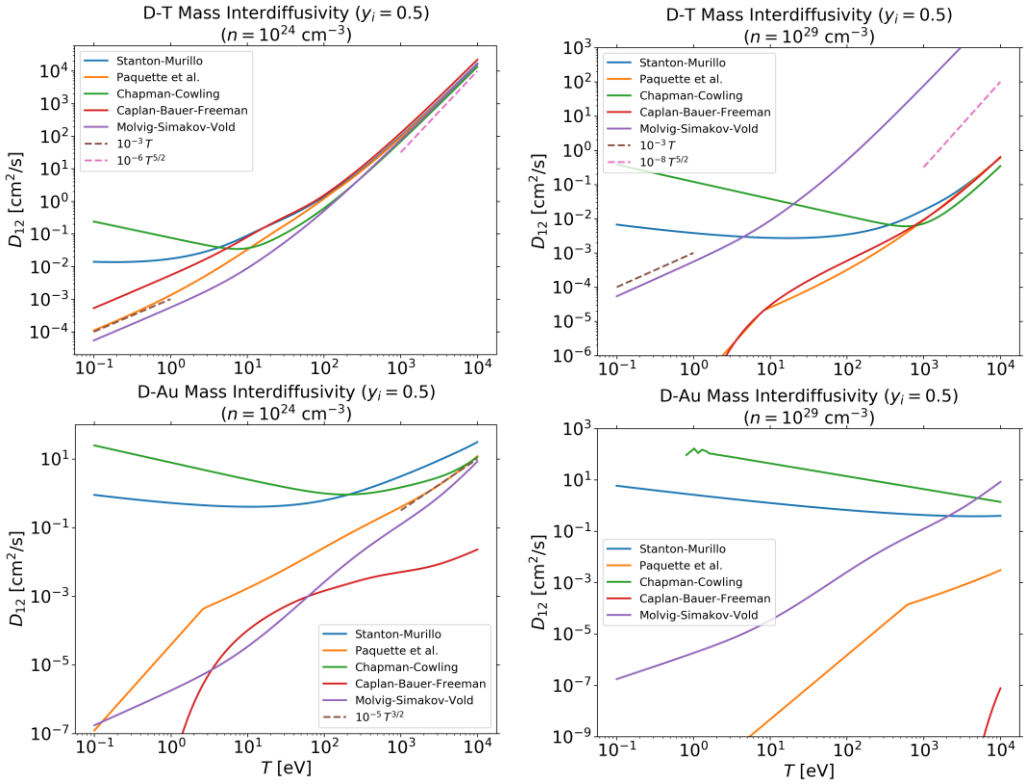

The binary viscosities are also increasingly divergent as asymmetry increases (Z_1 = 1 for D, Z_2 = 1 for T → 79 for Au) and number density increases ($n = 10^{24} \rightarrow 10^{29}$ cm^{-3})

- For D-T with $n = 10^{24}$ cm^{-3}, models agree well at high T, but can differ by orders of magnitude at low T (c.f., interdiffusivities)
- Except for D-T case with $n = 10^{24}$ cm^{-3}, models are quite different over entire temperature range
- For larger n, Molvig–Simakov–Vold model is orders of magnitude larger than other models at high T
- Stanton–Murillo and Paquette et al. models do not agree well at larger n and higher Z asymmetry
- Uncertainty in interdiffusivity and viscosity models increases with increasing Z asymmetry and number density at all T

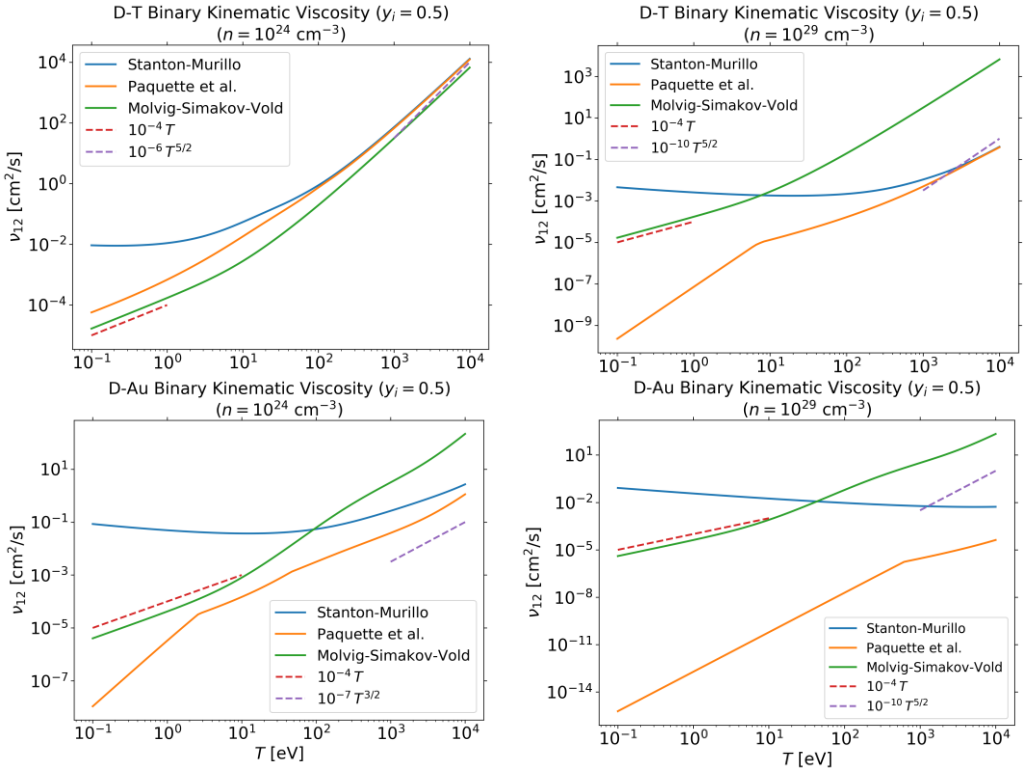

Applying the single-component models for self mass diffusivities to D with ρ = 1, 10, 100 g/cm^3 shows that model trends are similar (with some exceptions) as density increases

- Interdiffusivities decrease with increasing density
- Except for Chapman–Cowling model, scale as
  - $\propto T$ at low T
  - $\propto T^{5/2}$ at high T
- Except for original Ohta–Hamaguchi model, other models are in good agreement for $T >$ 0.1 keV
  - Rudd correction brings Ohta–Hamaguchi model into agreement at high temperatures
- Chapman–Cowling model predicts orders of magnitude larger values at lower T which decrease up to $T \sim$ 0.01 keV
- Caplan–Bauer–Freeman model diverges for 100 g/cm^3 below 0.001 keV

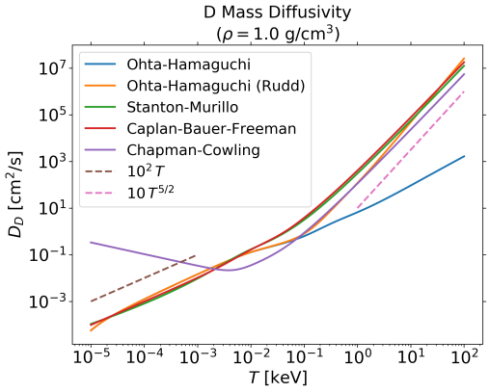

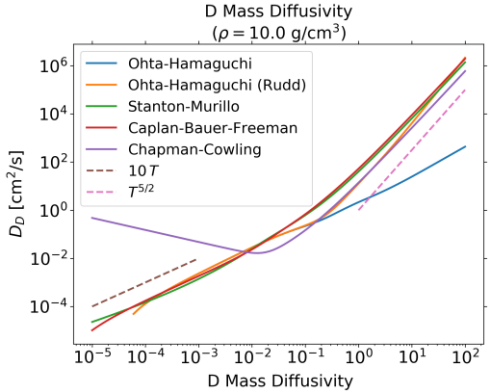

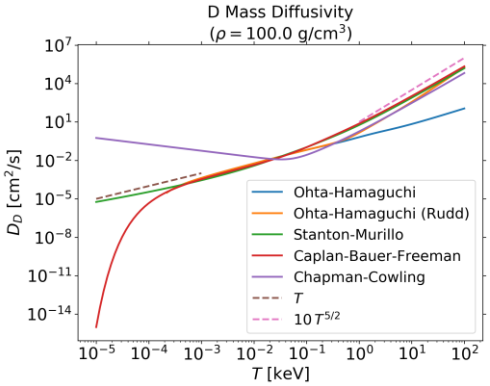

Except for the Chapman–Cowling and Caplan–Bauer–Freeman models, other models generally agree at *both* low and high temperatures

Applying the single-component models for self viscosities to D with ρ = 1, 10, 100 g/cm^3 shows that trends are similar to the mass diffusivities with increasing density

- Viscosities decrease with increasing density like interdiffusivities
- Except for Chapman–Cowling model, scale as $\propto T^{5/2}$ at high T
- Stanton–Murillo and Chapman–Cowling models are in very good agreement for $T > 0.1$ keV, diverging with increasing density and at lower temperatures
- Chapman–Cowling viscosity is > 10 orders of magnitude larger at lower T and decreases up to $T \sim 10$ keV
- Uncertainty in interdiffusivity and viscosity models increases with increasing Z asymmetry and number density, particularly at low T (i.e., in WDM regime)

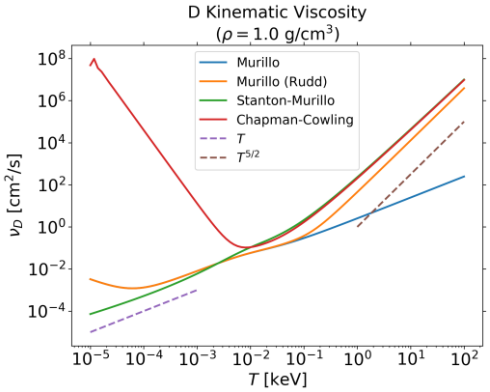

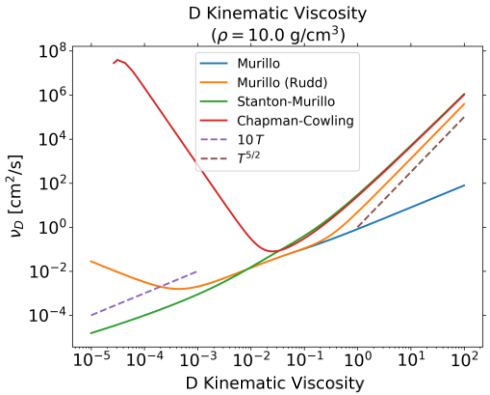

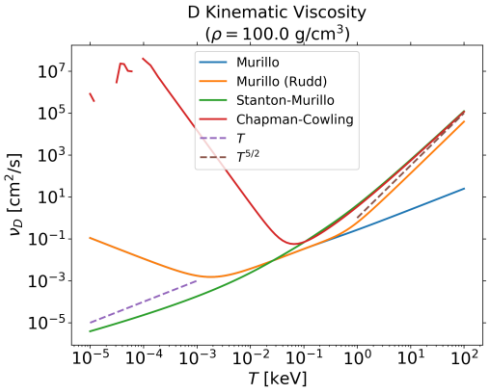

There are many outstanding challenges in warm dense matter and plasma transport modeling

- Vast parameter space {*Z*, *n*, *T*}
  - very sparse experimental data for constraining/validating models
  - MD cannot cover it all
  - need to assess range of validity of models and simulation data
  - need models that treat WDM to plasma regimes accurately, and are computationally tractable in complex multiphysics codes
- Transport coefficients for cases with > 2 species
  - empirical for > 2 species
  - very little data available for > 2 species
- Statistically-averaged coefficients in averaged approaches
  - nonlinear dependence of coefficients on *T* etc. implies that fluctuations could be important
  - including fluctuations is theoretically difficult, but may lead to nonlinear feedbacks between resolved/mean and unresolved/turbulent fields

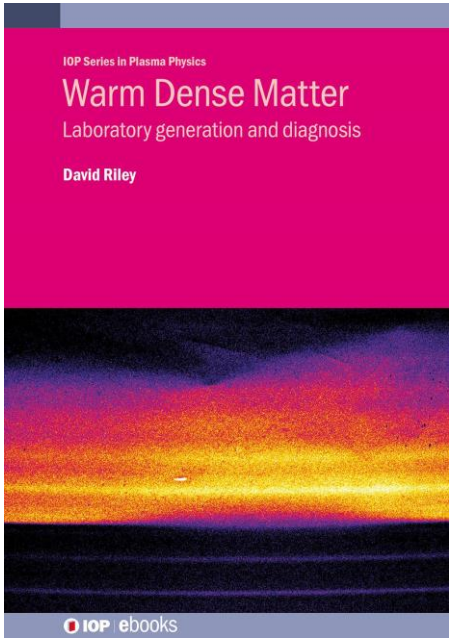

Special Topics issue in *Physics of Plasmas*: Charged-Particle Transport in High Energy Density Plasmas will include articles by participants of the Second Charged-Particle Transport Workshop, held at LLNL July 2023

Summary, conclusions, and future work

- A versatile `Jupyter/Python` package was developed for computing plasma and WDM transport coefficients
  - large number of single-component and binary kinetic and MD-informed models implemented
  - all required inputs calculated self-consistently, including mean ionization of mixtures
  - useful for comparing model predictions and developing physical insight into model physics
- Utility of package demonstrated by application to binary mixing with increasing charge asymmetry and increasing number density, and to single-component mixing
  - completely different models can agree closely at large T
  - models exhibit expected large T scalings, and coefficient values decrease with increasing asymmetry
  - significant differences in coefficient values and model trends are seen for increasing asymmetry and number density, and decreasing temperature (WDM regime)
- Future work includes adding other models and exploring validation
  - Simakov−Molvig (2016) model for ternary mixing, Kagan−Baalrud (2018) model based on effective potential theory, Daligault (2018) model for strongly-coupled systems, Stanton−Murillo (2021) model for electron transport, Lee−More−Desjarlais−Murillo conductivity model
  - explore modeling of ternary mixing
  - explore model hybridizations to bridge strongly- and weakly-coupled, and WDM and plasma, regimes

References

- Caplan, M. E., Bauer, E. B. & Freeman, I. F. 2022 Accurate diffusion coefficients for dense white dwarf plasma mixtures. *Monthly Notices of the Royal Astronomical Society Letters* **513**, L52−L56.
- Chapman, S. & Cowling, T. G. 1991 *The Mathematical Theory of Non-Uniform Gases: An Account of the Kinetic Theory of Viscosity, Thermal Conduction and Diffusion in Gases*, third edition, Cambridge University Press.
- Daligault, J. 2018 Collisional transport coefficients of dense high-temperature plasmas within the quantum Landau-Fokker-Planck framework. *Physics of Plasmas* **25**, 082703-1−082703-25.
- Fontaine, G., Brassard, P., Dufour, P. & Tremblay, P.-E. 2015 Metal Accretion onto White Dwarfs. I. The Approximate Approach Based on Estimates of Diffusion Timescales. *Proceedings of the 19th European Workshop on White Dwarfs*, edited by P. Dufour, P. Bergeron, and G. Fontaine, ASP Conference Series Vol. 493, 113−116.
- Molvig, K., Simakov, A. N. & Vold, E. L. 2014 Classical transport equations for burning gas-metal plasmas. *Physics of Plasmas* **21**, 092709-1−092709-19.
- Murillo, M. S. 2008 Viscosity estimates of liquid metals and warm dense matter using the Yukawa reference system. *High Energy Density Physics* **4**, 49−57.
- Ohta, H. & Hamaguchi, S. 2000 Molecular dynamics evaluation of self-diffusion in Yukawa systems. *Physics of Plasmas* **7**, 4506−4514.
- Paquette, C., Pelletier, C., Fontaine, G. & Michaud, G. 1986 Diffusion Coefficients for Stellar Plasmas. *Astrophysical Journal Supplement* **61**, 177−195.
- Rudd, R. E. 2012 Notes on the Yukawa Viscosity Model. Lawrence Livermore National Laboratory Report LLNL-MI-661976.
- Simakov, A. N. & Molvig, K. 2016 Hydrodynamic description of an unmagnetized plasma with multiple ion species. I. General formulation. *Physics of Plasmas* **23**, 032115-1−032115-16; Hydrodynamic description of an unmagnetized plasma with multiple ion species. II. Two and three ion species plasmas. Physics of Plasmas 23, 032116-1−032116-12.
- Stanton, L., Glosli, J. N. & Murillo, M. S. 2018 Multiscale Molecular Dynamics Model for Heterogeneous Charged Systems. *Physical Review X* **8**, 021044-1−021044-23.
- Stanton, L. & Murillo, M. S. 2016 Ionic transport in high-energy-density matter. *Physical Review E* **93**, 043203-1−043203-23.
- Stanton, L. & Murillo, M. S. 2021 Efficient model for electronic transport in high energy-density matter. *Physics of Plasmas* **28**, 082301-1−082301-11.
- Vold, E. L., Rauenzahn, R. M., Aldrich, C. H., Molvig, K., Simakov, A. N. & Haines, B. M. 2017 Plasma transport in an Eulerian AMR code. *Physics of Plasmas* **24**, 042702-1−042702-15.
- Vold, E., Yin, L. & Albright, B. J. 2021 Plasma transport simulations of Rayleigh−Taylor instability in near-ICF deceleration regimes. *Physics of Plasmas* **28**, 092709-1−092709-20.